

University of Groningen

## Strangeness photoproduction on the deuterium target

Shende, Sugat Vyankatesh

**IMPORTANT NOTE:** You are advised to consult the publisher's version (publisher's PDF) if you wish to cite from it. Please check the document version below.

*Document Version*

Publisher's PDF, also known as Version of record

*Publication date:*

2007

[Link to publication in University of Groningen/UMCG research database](#)

*Citation for published version (APA):*

Shende, S. V. (2007). *Strangeness photoproduction on the deuterium target*. s.n.

### Copyright

Other than for strictly personal use, it is not permitted to download or to forward/distribute the text or part of it without the consent of the author(s) and/or copyright holder(s), unless the work is under an open content license (like Creative Commons).

The publication may also be distributed here under the terms of Article 25fa of the Dutch Copyright Act, indicated by the "Taverne" license. More information can be found on the University of Groningen website: <https://www.rug.nl/library/open-access/self-archiving-pure/taverne-amendment>.

### Take-down policy

If you believe that this document breaches copyright please contact us providing details, and we will remove access to the work immediately and investigate your claim.

Downloaded from the University of Groningen/UMCG research database (Pure): <http://www.rug.nl/research/portal>. For technical reasons the number of authors shown on this cover page is limited to 10 maximum.

In this chapter the experimental set-up which was used for this work is discussed. The experiment has been carried out at the ELEktronen-Stretcher-Anlage (ELSA) Facility in Bonn. The TAPS and Crystal Barrel detector arrays and the tagger system are described in more detail.

### 3.1 ELSA Facility

The electron accelerator, ELEktronen-Stretcher-Anlage (ELSA), facility is available at the University of Bonn, Germany. It is capable of delivering a beam of polarized and unpolarized electrons up to 3.5 GeV. The electron beam is accelerated in three stages: a LINAC, a booster synchrotron and a stretcher ring. The schematic layout of ELSA is shown in fig.3.1. Initially the electron is accelerated up to 20 MeV or 26 MeV in LINAC 1 or LINAC 2, respectively. LINAC 2 produces the polarized electrons with approximately 80% polarization. For this work LINAC 2 was used because the polarized electron beam was needed for other experiments. In the next stage the electron beam was injected into the booster synchrotron. The latter accelerates the electron beam up to 1.6 GeV. In the last stage the electron beam enters into the stretcher ring. After the injection of several pulses from the booster synchrotron, the accumulated electron beam is accelerated by the stretcher ring up to the energy 3.5 GeV. In this ring the pulses of electrons are stretched in time in order to achieve a continuous beam for longer duration. The stretcher ring is filled during 2s and the maximum current is extracted over a period of 8s to the experimental area. A feedback loop

is set up for monitoring the beam intensity at the experiment and extraction is adjusted to achieve a stable maximized intensity. A more detailed discription of the ELSA layout can be found in [1].

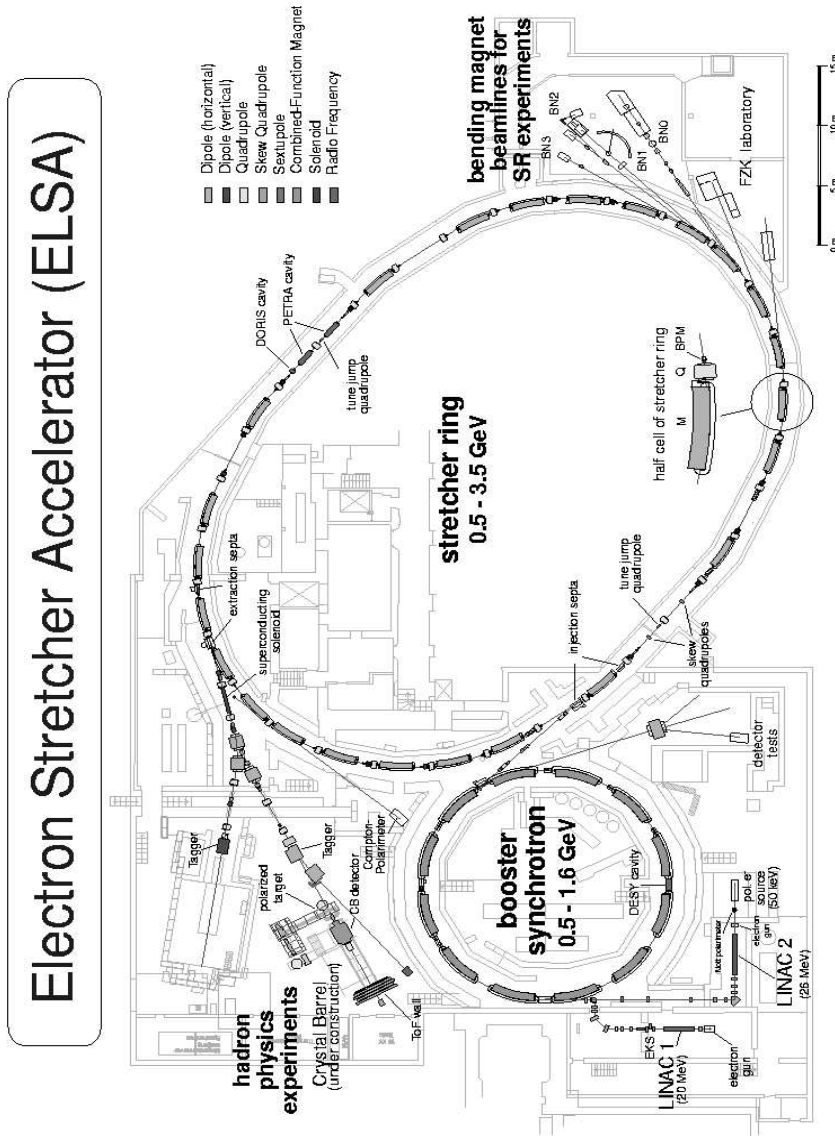
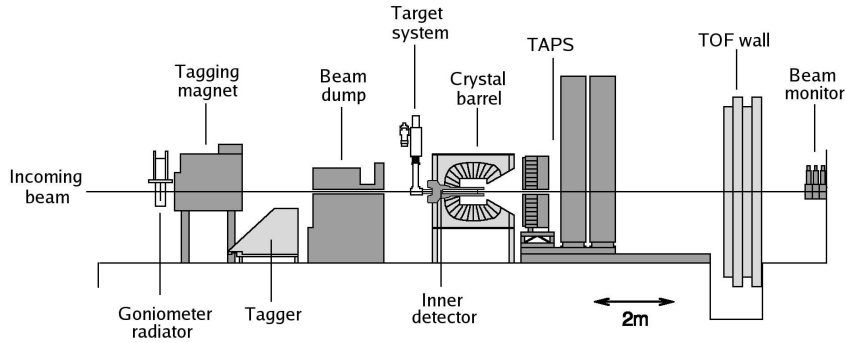


Figure 3.1: Schematic layout of ELSA electron accelerator at Bonn.



**Figure 3.2:** *Experimental beam line.*

### 3.1.1 Beam Line

The accelerated electron beam extracted from the stretcher ring enters into the experimental hall as shown in figure 3.2. As the beam enters into the hall it hits the radiator, producing bremsstrahlung photons. Then electrons are bent out from their path by a dipole magnet and their energy is measured using the tagger facility. The photon beam travels further and hits the target which is placed at the center of the Crystal Barrel (CB). Following a photon interaction on the target, exit channel photons from all possible reactions are detected by the combination of CB and TAPS. The photons which do not interact with the target are measured by the Gamma Veto detector at the end of the beam line. The Gamma Veto monitors the position and flux of the photon beam.

### 3.1.2 Tagger

The electron beam from the ELSA accelerator is converted into a photon beam by a bremsstrahlung reaction on the radiator. The energy spectrum of the emitted photons is given in first approximation by

$$\Phi \propto \frac{1}{E_\gamma} \quad (3.1)$$

The half-angle  $\theta$ , between the bremsstrahlung photon and the incoming electron beam for relativistic energies is given by [15]

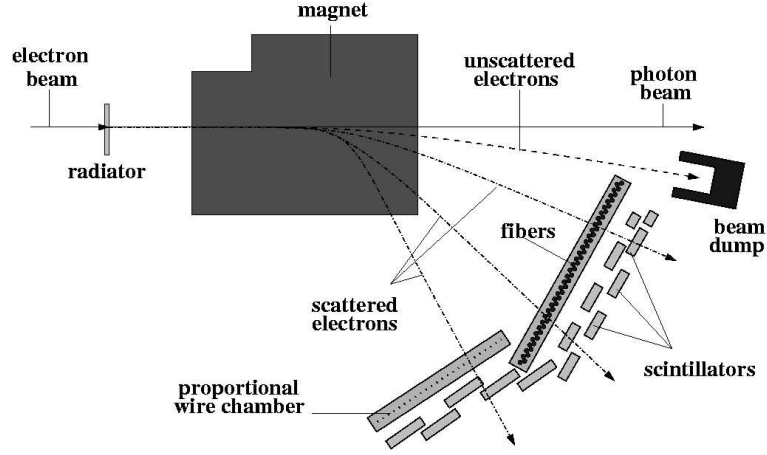


**Figure 3.3:** *The schematic layout of the Tagging system.*

$$\langle \theta^2 \rangle^{\frac{1}{2}} = \frac{1}{\gamma} = \frac{m_e c^2}{E} \quad (3.2)$$

where the half-angle  $\theta$  is in rad. For a photon energy of 1.5 GeV the above formula gives an half-angle of 0.3 mrad, which means the radiation is emitted in a very narrow cone along the incoming electron beam direction. After the electrons are bent out from the photon beam, their momentum is measured in order to calculate the photon energy on an event by event basis.

The schematic layout of the tagging system is shown in figure 3.3. It consists of 14 overlapping plastic scintillator bars each fitted with a photo multiplier on both ends. To improve the energy resolution, a second layer of scintillating fibers is added on the higher electron energy side. A proportional wire chamber is added in such a way that it overlaps the plastic scintillator bars which are on the lower electron energy side. The fiber detector system consists of 480 plastic scintillation fibers arranged in two layers, slightly offset with respect to each other in such a way that each fiber partly overlaps two fibers in the other layer. The fibers are connected to a multiple-anode photo multiplier tube. The bars cover the photon energy range between 22% and 92% of the incoming electron beam energy. The fibers cover the range between 18% and 80%, as the fibers covers more area beyond the edge of the last scintillator bar that is located closest to the photon beam. The proportional wire chamber is not used in this work as its energy range is outside of the region of interest.

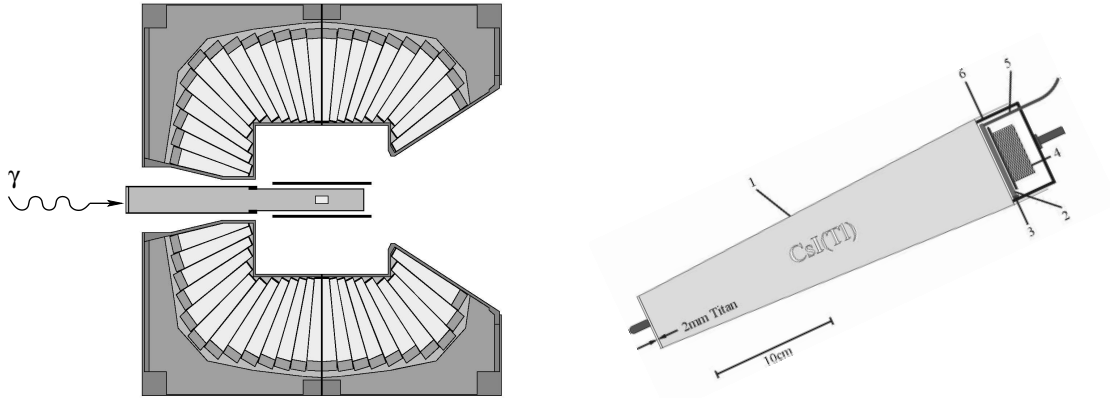


**Figure 3.4:** Left: The Cross sectional view of the Crystal Barrel detector. Beam is entering from the left. The target area, indicated in the center, is surrounded by the Inner detector. Right: Cross section of CsI(Tl) module: 1)0.1mm titanium can, 2)wavelength shifter, 3)photo diode, 4)preamplifier, 5)light fiber, 6)brass cover.

### 3.1.3 Target

The target consists of a 5 cm long kapton foil tube of radius 1.5 cm. The kapton thickness is 0.125 mm. The target is filled with liquid deuterium, but it can also be filled with liquid hydrogen. The target is situated inside the aluminum beam-pipe. A heat exchanger is used to cool the deuterium in the target. For the experiments on solid targets, the cell was empty and pulled backwards to make room for the solid-target holder.

### 3.1.4 Crystal Barrel

The Crystal Barrel calorimeter consists of 1290 CsI crystals, doped with thallium. The crystals are arranged in a cylindrical shape covering polar angles from  $30^\circ$  to  $168^\circ$ . The arrangement is shown in figure 3.4 (left), and the individual crystal module is shown in figure 3.4 (right). Each crystal is 30 cm long, corresponding to 16 electromagnetic radiation lengths. On top of each crystal a photo diode is mounted. A wavelength shifter is sandwiched between crystal and photo diode to convert the light from the crystal into a suitable wavelength range. The photo diode signal is then preamplified before it is sent to the readout electronics. Each crystal was suspended by an outside support structure. For this purpose, the crystals and associated electronics are enclosed in titanium cans of 0.1 mm thickness. An optical fiber is attached to each crystal, allowing laser light of a

known frequency to be guided into the crystal for calibration purposes. As the light output is very sensitive to the detector temperature and the CsI crystals are very hygroscopic, the whole detector is kept slightly above room temperature. The crystals are arranged in 23 rings as shown in figure 3.4, at an average distance of 300 mm from the target. Each ring contains 60 detectors, except the three most backward rings which contain only 30 crystals. The position resolution that can be obtained is 20 mrad (40 mrad for the backward rings). The energy resolution is 2.8% (at 1 GeV). A more detailed description can be found in [51].

### 3.1.5 Inner detector

In order to identify the charged particles inside the Crystal Barrel an array of scintillating fibers (Scifi) was installed. These fibers are 200 mm in length and arranged parallel to the beam line surrounding the target covering polar angles from  $28^\circ$  to  $172^\circ$ . The three layers of scintillating fibers are glued to a 0.8 mm epoxy composite support. Each fiber has a diameter of 2 mm. The outer layer has a diameter of 128 mm and contains 191 fibers. The middle layer contains 165 fibers oriented at an angle of  $+25^\circ$  with respect to the first layer and has a diameter of 122 mm. The inner layer has a diameter of 116 mm and contains 157 fibers rotated by  $-25^\circ$ . The fact that the layers are crossing each other at an angle makes it possible to determine all three spatial coordinates of a charged-particle hit. The hypothetical angular resolution of the Inner detector in the case of a point target is  $1^\circ$ . Due to the length of the target the resolution in this experiment was around  $10^\circ$ . The produced scintillation signal can identify minimum ionizing charged particles with an efficiency close to 100%. The deposited energy is not recorded in the present experiment, only the time and position of a charged hit has been measured. More details can be found in [52].

### 3.1.6 TAPS Detector

The TAPS detector is an electromagnetic calorimeter designed to detect individual photons. It consist of 528 detector modules made up of  $BaF_2$  scintillation material. Each individual module has an hexagonal shape with inscribed cone diameter of 59 mm. The last 25 mm are machined cylindrically in diameter( $\phi=52$  mm) to facilitate the connection to the photo multiplier. The length of each module is 250 mm which corresponds to 12 electromagnetic radiation lengths.

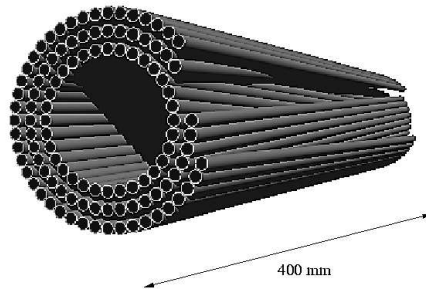


**Figure 3.5:** Inner detector with three layers of fibers oriented in different directions.

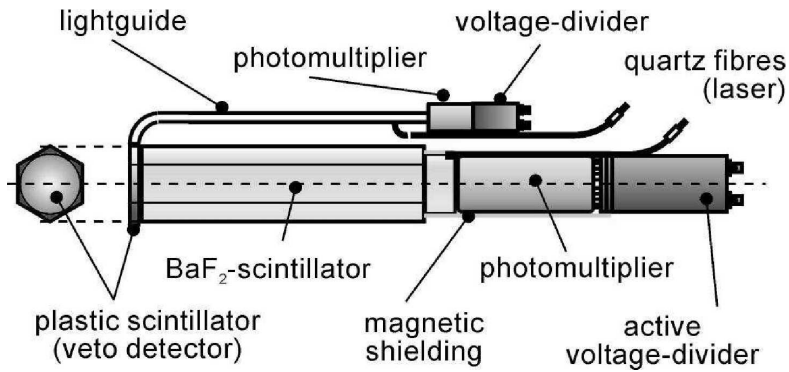


**Figure 3.6:** A single module of the TAPS detector.

Each crystal is wrapped with eight layers of  $38\ \mu\text{m}$  PTFE and an additional layer of aluminum foil as UV-reflector and coupled optically to the quartz window of the photo multiplier (Hamamatsu R2059-01). The whole assembly including the photo multiplier base is covered by 0.2 mm thick light-tight PVC tube, in order to get sufficient mechanical strength. The single module is shown in figure 3.6. A more detailed description can be found in [53].

In this experiment the  $\text{BaF}_2$  modules are arranged in the so called super cluster geometry as shown in figure 3.7 and positioned at the forward angle opening of the Crystal Barrel detector as shown in figure 3.2 at a distance of 1.18m from the center of the target. TAPS covers the forward polar angles from  $5.8^\circ$  to  $30^\circ$ . Other experiments were conducted simultaneously and some of these involved channels decaying into only a few photons. The possibility of very high energy photons hitting TAPS had to be considered. The gain of the photo multiplier was adjusted such that the current output of the photo multiplier for photons of 3 GeV was still low enough to be processed by the readout system. The energy resolution attained with this setup over the incident photon energy



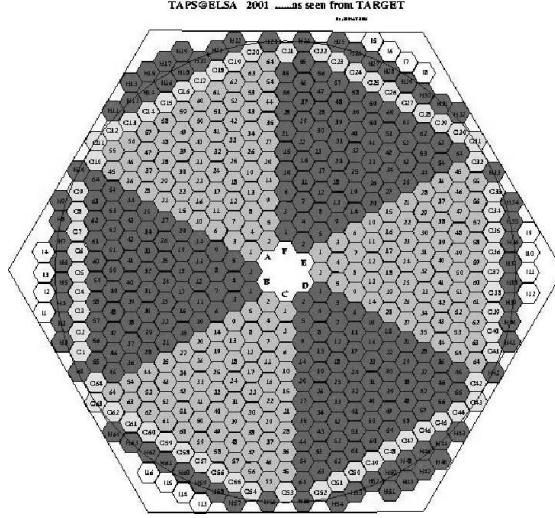


**Figure 3.7:** Front view of TAPS detector.

range from 200 to 800 MeV is 2.5% [54]. The position resolution for photons was found to be 20 mm from Monte Carlo simulations using the GEANT [55] package and the proper detector geometry.

$BaF_2$  has a special property. It has two light components (different wavelengths) with different decay times. The relative amount of these light components depends on the ionization density of the incident radiation. This intrinsic property of  $BaF_2$  is very useful to separate photons and nucleons using the pulse-shape technique. The pulse shape is the sum of different components, some with fast and some with slow decay times. Since the photons and protons interact differently with the crystal, their pulse shape response contains these components in different admixtures. The pulse shape for protons has a larger component with a long decay time compared to the photon. To obtain experimental data which allows the pulse shape to be determined, one integrates the signal twice, once within a narrow gate (50 ns) and once within a wide gate (2  $\mu$ s), as shown in figure 3.8. If one plots the integral over the narrow gate ( $E_{narrow}$ ) versus the integral over the wide gate ( $E_{wide}$ ), the protons and photons form two distinct bands. Although a good separation is achieved over most of the energy range, this method fails at higher energies where the proton pulse shape comes too close to the photon pulse shape. For the selection of events belonging to the reaction channel of interest, this information is therefore only used to check how well the channel is selected by the kinematical constraints.

In front of each  $BaF_2$  crystal an hexagonal plastic scintillator (NE 120A) is

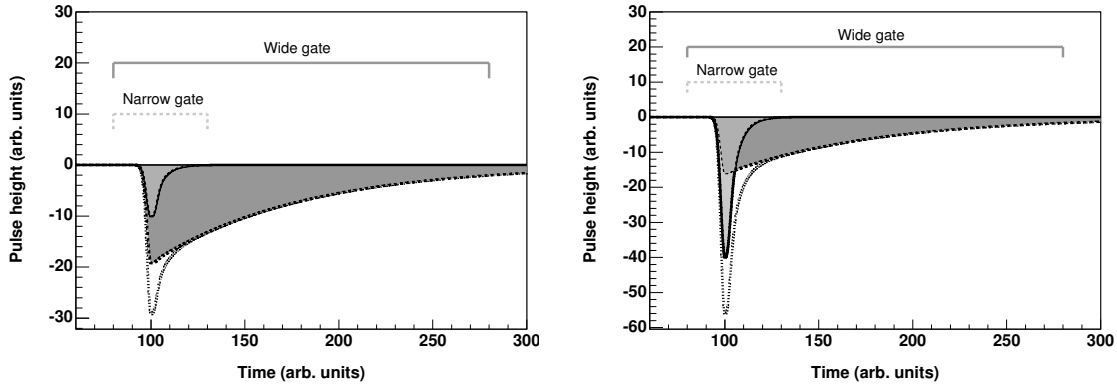


**Figure 3.8:** *Left: A schematic drawing of the pulse shape for protons in TAPS. Right: A schematic drawing of the pulse shape for photons in TAPS. The stronger narrow-gate component for photons makes it possible to differentiate protons from photons.*

placed with the same diameter as the crystal and a thickness of 5 mm, called charged-particle veto (CPV) detectors, where the veto feature is not used in this experiment. It provides additional information on charged particles which can be helpful in particle identification. Each CPV is connected to a multiple anode photo multiplier tube on the edge of the detector-array via a long plastic fiber to minimize the amount of matter in front of the detector. More information on the design of the CPV system can be found in [56].

### 3.1.7 Time of flight wall

The Time of Flight (TOF) wall provides additional information for the particles passing through the TAPS detector. It consists of four planes of plastic scintillators. Each plane is built up of 15 scintillator bars which are 20 cm high and 3 m long such that the complete plane covers an area of 3 by 3 meter. The thickness of the scintillators is 5 cm. In the first and third planes, the orientation of the bars is horizontal, in planes 2 and 4 it is vertical. For this experiment the TOF detector information was not used.

### 3.1.8 Beam monitor

At the end of the beam line the Gamma Veto detector is located which measures those photons that passed through the target without undergoing an interaction.

The number of photons arriving at this detector in coincidence with those seen at the tagger gives the photon flux through the target. The other use of this detector is to provide a way to measure the beam position at the end of the setup and thereby providing a means to check the beam alignment.

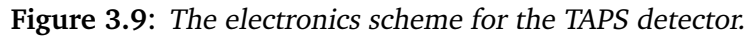
## 3.2 Data acquisition

### 3.2.1 Crystal Barrel

The signals coming from the Crystal Barrel photo diodes are passed via shapers to the Charge to Digital Converters(QDC), which integrate the total charge present in the signal in two energy ranges. The QDC's contain two different capacitors and the incoming signal is split in a ratio of 1 to 8 between them. The internal logic then decides which charge to digitize. If the signal is small the charge on the capacitor with the highest charge will be integrated. If the signal is large the other capacitor with the lowest charge will be integrated. In this way each QDC covers two different ranges, up to 200 MeV, and up to 2 GeV. Each range is digitized into 12 bits and an additional bit is set to specify the used range. The QDC's are readout by a VMIC computer on a VME compatible board running Linux. The interface to the VME backplane is accomplished via Tundra Universe PCI-VME interface. Two such modules collect the digitized data from the QDC's where one module is responsible for the upstream and one for the downstream Crystal Barrel half. The two VMIC computers each build their subevent and send this via TCP/IP to a central event builder. More information on data handling and transport can be found in [57].

### 3.2.2 Tagger

All 480 fibers of the scintillating fiber tagger are connected to Constant Fraction Discriminators (CFD's) close to the detector. From there the resulting logic signals are sent outside the experimental hall through delay lines and passed through a passive splitter. From the splitter the signals are fed to a multi-hit Time to Digital Converter (TDC) with a resolution of 64 ps/ch and to a scaler. The TDC's are used in common-stop mode, where the experiment trigger provides the stop signal. Both the TDC's and the scalers are mounted on top of



### 3.2.3 Inner detector

### 3.2.4 TAPS

<sup>1</sup>COMPASS Accumulate Transfer and Control Hardware [58]

has to be delayed to allow time for the trigger to be formed, therefore it is passed through 60 m long cables and a delay box of 500 ns. It is then connected to a QDC to integrate the signal within two different gates, one narrow (50 ns) and one wide (2  $\mu$ s) gate. This allows to perform pulse-shape identification. The second and third signals are connected to two Leading Edge Discriminators(LED's), the LED-low and the LED-high, which are used to form the TAPS pretrigger. The fourth signal from the split is used for timing, gate generation for the QDC's, and zero suppression. This signal is passed through a Constant Fraction Discriminator(CFD) which provides a logic signal for timing purposes. The output of this CFD is then taken out of the experimental area and passed through a daisy chain. The first link on the daisy chain is used as the input for a gate generator (RDV), which provides the QDC's with the two gates mentioned previously. The second link provides the stop-input for the TDC's, which were operated in common-start mode and were started by the trigger signal. The third and final link is again a bit register. This register is monitored by the acquisition system, and only detectors which have a bit set will be read out. In other words, only detectors in which enough energy was deposited to reach the CFD threshold will be read out. The average CFD threshold was adjusted around 10-15 MeV.

In addition to the signal input, the splitters also provide a 1 Hz pulser to all CFD's, so that a gate was generated without a signal being present. This method allows to monitor the position of the pedestals in the QDC spectra.

### 3.3 Trigger

Since the data acquisition system is not fast enough to record everything that is seen by the detector and because many events come from processes like photon conversion, events have to be selected on-line. In order to make such selection some trigger conditions have to be implemented. The main trigger used for this experiment consists of two levels. In the first level the decision is made whether the measurement is interesting enough to start the digitization of all measured values. This decision has to be made as fast as possible. During the digitization more time is available during which the second-level trigger decides whether or not to read out the event. Because of the longer available time span the second-level trigger may be more complex. The analog signals from TAPS pass through a delay line of 300 ns, thus the decision has to be made and passed to the readout electronics within that time. The signals from the Crystal Barrel

can not be used for the first-level trigger. Since the Barrel crystals are equipped with photo diodes, the signal rise time is too slow ( $2\ \mu\text{s}$ ) to provide the first-level trigger. Therefore the first-level trigger is completely provided by TAPS, which is equipped with fast photo multiplier tubes. The second level trigger is used to determine whether the digitized signals need to be read out for further processing.

### 3.3.1 First-level trigger

To build the trigger, the signals coming from two Leading Edge Discriminators (LED's), LED-low and LED-high, are used. Three different kinds of first-level triggers or “pretriggers” have been used. For the first pretrigger, LED-low mult 2, two hits in the TAPS detector above the LED-low threshold were required. For this purpose the supercluster setup is divided into 8 segments as shown in figure 3.11. The signals from each segment are then fed to an MLU (Memory Lookup Unit) which is programmed to select a multiplicity of at least two. A second pretrigger, LED-low OR, is made by requiring only a multiplicity of one with suitable downscaling of the resulting high trigger rate. The third pretrigger, LED-high OR, uses only one hit in TAPS determined by the LED-high signals. The TAPS detector is again subdivided in segments, but this time following a different layout as shown in figure 3.10.

### 3.3.2 Second-level trigger

The second-level trigger is based on the number of clusters found in the FAST Cluster Encoder (FACE). It is an array of logic units, connected to the output of the Crystal Barrel modules, which counts the number of clusters on-line. In this experiment two different second-level triggers have been used for different data-taking periods. The first case requires at least one cluster to be identified in the Crystal Barrel whenever a LED-high OR pretrigger was given by TAPS. For the second case, two clusters are required in the FACE for the LED-high pretrigger. For LED-low multiplicity 2 trigger no additional conditions were imposed. If the second-level trigger approves the event, all measured signals are digitized, read and sent to data storage. The trigger rates are adjusted by changing the LED thresholds and the beam intensity in order to maintain a system dead-time of 50%.

Apart from First-level trigger and Second-level trigger an additional trigger

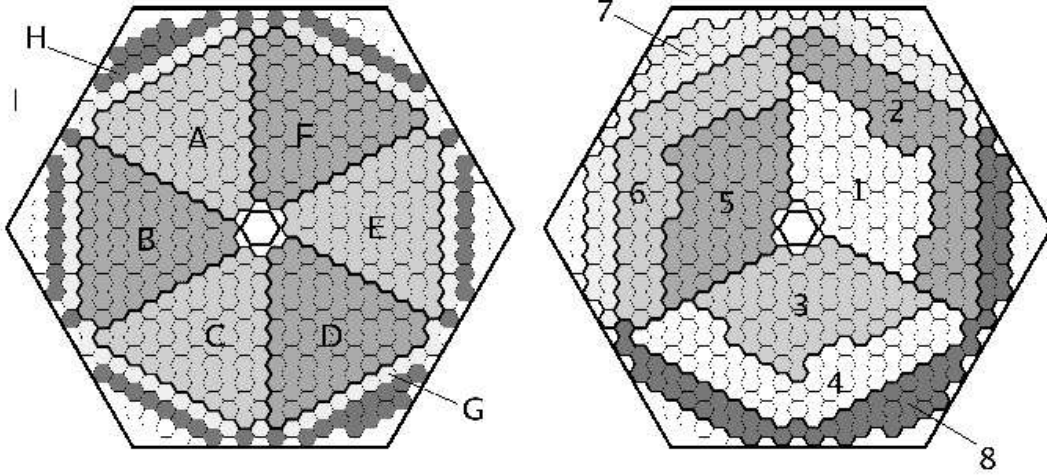


**Figure 3.10:** Segmentation of the TAPS detector for the LED high multiplicity 1 detector for the LED low multiplicity 2 pretrigger.

**Figure 3.11:** Segmentation of the TAPS detector for the LED low multiplicity 2 pretrigger.

was built to use TAPS in a stand alone mode. This trigger was mostly used for debugging and calibration purposes using cosmic radiation.